

Investigating tumour cycling hypoxia with resting state MRI: relationship with systemic changes and influence of noise

M. R. Gonçalves^{*1}, S. Walker-Samuel^{*1}, S. P. Johnson², R. B. Pedley², and M. F. Lythgoe¹

¹UCL Centre for Advanced Biomedical Imaging, Division of Medicine and Institute of Child Health, London, London, United Kingdom, ²UCL Cancer Institute, London, London, United Kingdom

^{*}joint first authors

Target audience: Researchers interested in cancer studies, particularly cycling tumour hypoxia.

Introduction: Solid tumours have been observed to exhibit regions of transient, cycling hypoxia and subsequent reoxygenation due to spontaneous fluctuations in blood flow and oxygenation [1, 2]. This has been shown to contribute to resistance to chemotherapy [3] and radiotherapy [4], as well as tumour progression and development of metastatic disease [5, 6]. R_2^* ($=1/T_2^*$) estimates from gradient echo MRI (GRE-MRI) have been employed in the study of tumour cycling hypoxia due to its dependence on deoxygenated hemoglobin [1, 7]. However, the influence of systemic changes in blood oxygenation on tumour R_2^* fluctuations has not been directly investigated, particularly in anaesthetised animals, in which both properties can vary. In this study, we have modelled systemic (arterial) and tumour vasculature as shown in Fig. 1, in which the tumour is influenced by systemic changes in oxygenation, but can also modify this parameter. We have measured resting state R_2^* fluctuations in the tumour with simultaneous systemic blood O_2 saturation, in order to assess their relationship. Furthermore, we estimated the influence of measurement noise on tumour R_2^* fluctuations.

Methods: 5×10^6 SW1222 ($n=6$) or LS174T ($n=5$) colorectal carcinoma cells were injected subcutaneously into MF1 *nu/nu* mice. After growing to an approximate volume of 500mm^3 , tumours were imaged on a 9.4T Agilent VNMRS 20cm horizontal-bore system, with a 39mm birdcage coil, using a multi-slice, multi-gradient echo (GEMS) sequence. Mice were anaesthetised using isoflurane (1.25% in medical air). Respiratory frequency varied between 43-92 breaths/min and temperature was maintained at 36.7°C . A scan of 60min duration was performed to evaluate spontaneous fluctuations in tumour R_2^* ($=1/T_2^*$). Simultaneously, arterial hemoglobin O_2 saturation ($O_{2\text{sat}}$) was measured by pulse oximetry on the thigh (MouseOx®, Starr Life Sciences Corp., Oakmont, PA). Voxel-wise post-processing included: i) Resting state R_2^* maps, that depict the standard deviation of unchallenged R_2^* time courses in each voxel. ii) $RS_{(SD)}/\text{uncertainty}$ maps represent voxels whose R_2^* amplitude changes are above the uncertainty due to background noise, which was estimated using a Markov Chain Monte Carlo (MCMC) approach [8]. iii) **p-value** maps show the Pearson's correlation significance between R_2^* time courses and O_2 saturation ($O_{2\text{sat}}$, R_2^*). **GEMS parameters:** SPGR sequence with $TR=59.62\text{ms}$, 5 echoes, $TE_1=2\text{ms}$, echo spacing=2ms, 5 slices, 64×64 matrix, voxel volume $312 \times 312 \times 1500\mu\text{m}$, $FA=20^\circ$.

Results: We present example maps of i) Resting State R_2^* , ii) $RS_{(SD)}/\text{uncertainty}$ and iii) $p(O_{2\text{sat}}, R_2^*)$, as well as arterial O_2 saturation and averaged ΔR_2^* timecourses. Resting State R_2^* maps show clear variations in R_2^* (Fig. 2a). Maps of the ratio of the variance in temporal R_2^* fluctuations and measurement uncertainty (from MCMC analysis) are shown in Fig. 2b, in which voxels with $RS_{(SD)}/\text{uncertainty} > 1$ indicate regions within the tumour with temporal fluctuations greater than measurement noise level (percentage of voxels above noise level was 50.3% and 71.1% for SW1222 and LS174T tumours, respectively). Fig. 2c shows the p-values obtained from the correlation between systemic arterial hemoglobin O_2 saturation (depicted in Fig. 2d) and individual voxel R_2^* timecourses. We observed clusters of voxels with R_2^* significantly correlated ($p < 0.01$) with systemic O_2 saturation (arrow), and Fig. 2e shows the averaged ΔR_2^* for the voxels with $p(O_{2\text{sat}}, R_2^*) < 0.01$, showing a clear correspondence with the $O_{2\text{sat}}$ curve. However, other regions with significant R_2^* fluctuations showed no correlation with systemic $O_{2\text{sat}}$, and were consequently categorised as exhibiting tumour-specific fluctuations. According to this analysis, the mean percentage of tumour voxels displaying tumour-specific fluctuations was 38.7% and 57.3% for SW1222 and LS174T tumours, respectively ($p=0.18$, Mann-Whitney U test); the percentage of voxels displaying systemic only R_2^* fluctuations was 17.5% and 15.2% for SW1222 and LS174T, respectively ($p=0.93$, Mann-Whitney U test) (Fig. 3).

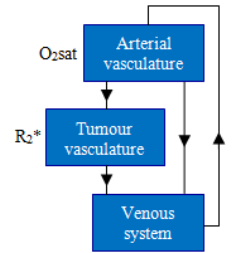


Fig. 1 – Schematic of the influence of the system on tumour vasculature.

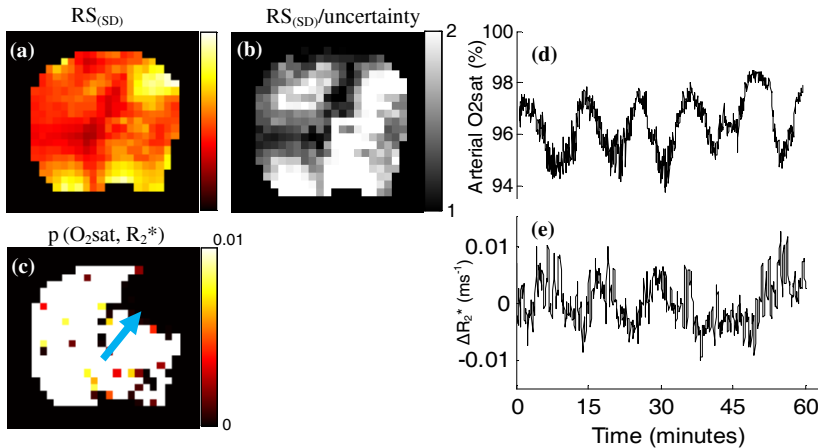


Fig. 2 – LS174T tumour xenograft. (a) Resting State standard deviation – $RS_{(SD)}$ map of R_2^* fluctuations. (b) Map of $RS_{(SD)}$ voxels above noise uncertainty ($RS_{(SD)}/\text{uncertainty} > 1$). (c) p-values from Pearson's correlation between $O_{2\text{sat}}$ and R_2^* . (d) Systemic arterial hemoglobin $O_{2\text{sat}}$ (%). (e) Mean R_2^* for the voxels with $p(O_{2\text{sat}}, R_2^*) < 0.01$.

Discussion & Conclusion: Maps of resting state R_2^* fluctuations included tumour voxels in which the fluctuations were greater than the uncertainty associated with measurement noise. Within these regions, it was found that $RS_{(SD)}$ maps show regions of high R_2^* amplitude variations that correlate significantly with systemic changes in blood oxygenation. However, we also observed fluctuations that were not significantly correlated with systemic oxygenation changes, which were considered to be related to localised (tumour-specific) changes in oxygenation. One limitation of this method is its inability to detect systemic effects in pixels displaying a combination of systemic and tumour-specific effects. This limitation could potentially be addressed using independent component analysis techniques. LS174T tumours displayed a higher percentage of tumour-specific fluctuating voxels than SW1222 tumours, although this difference was not statistically significant. We also found no difference between tumour types when analysing the percentage of systemic fluctuating voxels. These results suggest that, even though LS174T tumours are less vascularised and less perfused than SW1222 tumours [9], they show no differences with regard to R_2^* spontaneous fluctuations.

Acknowledgements: This work was carried out as part of King's College London and UCL Comprehensive Cancer Imaging Centre CR-UK & EPSRC, in association with the MRC, DoH and British Heart Foundation (England).

References: [1] Baudelet C, et al., *Phys. Med. Biol.* 49: 3389-411. [2] Brown JM, *Br. J. Radiol.* 52: 650-6. [3] Durand RE, *Cancer and Metastasis Rev.* 20: 57-61. [4] Chaplin DJ, et al., *Cancer Res.* 47: 597-601. [5] Hill RP, *Cancer and metastasis Rev.* 9:137-47. [6] Cairns RA, et al., *Cancer Res.* 61:8903-8. [7] Baudelet C, et al., *NMR Biomed.* 19:69-76. [8] Walker-Samuel S, et al., *Magn. Res. Med.* 63(3):914-21. [9] Folarin A, et al., *Microvascular Res.* 80: 89-98.

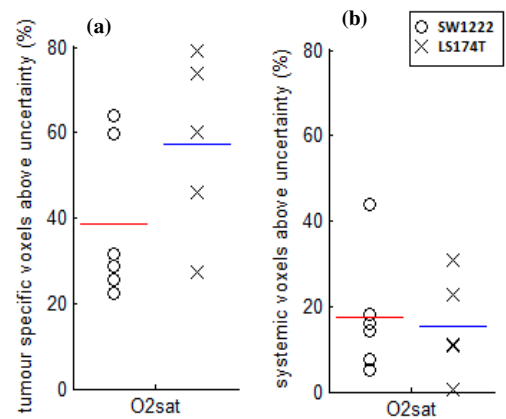


Fig. 3 – Percentage of (a) tumour-specific fluctuating voxels and (b) systemic fluctuating voxels, when compared to the $O_{2\text{sat}}$ curve.